Expression and regulation of GPAT isoforms in cultured human keratinocytes and rodent epidermis

Biao Lu,[1],* Yan J. Jiang,[1,2],† Peggy Kim,† Art Moser,† Peter M. Elias,§ Carl Grunfeld,† and Kenneth R. Feingold[†]

Department of R&D,* System Biosciences, Mountain View, CA 94043; Metabolism Section[†] and Dermatology,§ Department of Veterans Affairs Medical Center, University of California San Francisco, San Francisco, CA 94121

Abstract Phospholipids are required for epidermal lamellar body formation. Glycerol 3-phosphate acyltransferases (GPATs) catalyze the initial step in the biosynthesis of glycerolipids. Little is known about the expression and regulation of GPATs in epidermis/keratinocytes. Here, we demonstrate that GPAT 1, 3, and 4 are expressed in epidermis/keratinocytes, whereas GPAT2 is not detected. In mouse epidermis, GPAT 3 and 4 are mainly localized to the upper layers whereas GPAT1 is found in both the upper and lower layers. GPAT1 and 3 mRNA increase during fetal rat epidermal development. No change in GPAT expression was observed in adult mice following acute permeability barrier disruption. Calcium-induced human keratinocyte differentiation increased GPAT3 mRNA whereas both GPAT1 and 4 mRNA levels decreased. In parallel, total GPAT activity increased 2-fold in differentiated keratinocytes attributable to an increase in N-ethylmaleimide (NEM) sensitive GPAT activity localized to microsomes with little change in NEM resistant activity, consistent with an increase in GPAT3. Furthermore, PPARγ or PPARδ activators increased GPAT3 mRNA, microsomal GPAT activity, and glycerol lipid synthesis without affecting the expression of GPAT1 or 4. Finally, both PPARγ and PPARδ activators increased GPAT3 mRNA via increasing its transcription. Thus, multiple isoforms of GPAT are expressed and differentially regulated in epidermis/keratinocytes.—Lu, B., Y. J. Jiang, P. Kim, A. Moser, P. M. Elias, C. Grunfeld, and K. R. Feingold. **Expression and regulation of GPAT isoforms in cultured human keratinocytes and rodent epidermis.** *J. Lipid Res.* 2010. **51:** 3207–3216.

Supplementary key words glycerol-3-phosphate acyltransferase • fatty acids • phospholipid • permability barrier

The principal function of the epidermis is to provide a protective barrier against transcutaneous water loss, which is essential for survival in a terrestrial environment. This permeability barrier is localized to the stratum corneum (SC), the outermost layer of the epidermis (1). This permeability barrier is mediated by extracellular lipids, primarily cholesterol, ceramides, and free fatty acids, which are delivered to the extracellular spaces of the SC by the secretion of lamellar body contents by differentiated keratinocytes (1). Lamellar bodies contain cholesterol, glucosylceramides, and phospholipids, and following lamellar body secretion the glucosylceramides are metabolized to ceramides, a process catalyzed by the enzyme β-glucocerebrosidase, and the phospholipids are metabolized to free fatty acids, a reaction catalyzed by secretory phospholipases (1–4). The formation of lamellar bodies by keratinocytes requires the prior synthesis of sufficient quantities of these three lipids in keratinocytes. Pertinently, disruption of the permeability barrier leads to a marked increase in epidermal cholesterol, ceramide, and fatty acid synthesis, which enhances the formation of lamellar bodies (1, 5). Conversely, inhibition of cholesterol, ceramides, or fatty acid synthesis in the epidermis impairs the formation of lamellar bodies, leading to the decreased delivery of lipid to the extracellular spaces of the SC and impaired permeability barrier function (6–8).

Abbreviations: 1-acyl-*sn*-glycerol-3-phosphate acyltransferase, AGPAT; AT, all-*trans* retinoic acid; 9-*cis*, 9-*cis* retinoic acid; Cig, ciglitazone; CHK, cultured human keratinocyte; DGAT, acyl-CoA: diacylglycerol acyltransferase; ER, endoplasmic reticulum; GPAT, glycerol-3-phosphate acyltransferase; GW, GW 610742X; LB, lamellar body; LXR, liver X receptor; mGPAT, microsomal GPAT; NEM, N-ethylmaleimide; PC, phosphatidylcholine; PE, phosphatidylethanolamine; PPAR, peroxisome proliferator-activated receptor; 22(R), 22(R)-OH-cholesterol; qPCR, quantitative real-time PCR; PS, phosphatidylserine; RAR, retinoic acid receptor; RXR, retinoid X receptor; SB, stratum basale; SC, stratum corneum; SG, stratum granulosum; SREBP, sterol-regulatory element binding protein; SS, stratum spinosum; TEWL, transepidermal water loss; TO, TO 901317; Tro, troglitazone; WT, wild type; WY, WY14643.

[1] These authors contributed equally to this work.
[2] To whom correspondence should be addressed.
  e-mail: yan.jiang@med.va.gov

Phospholipid-derived fatty acids are essential for the formation of the epidermal permeability barrier (1). Whereas much is known about the regulation and the role of sphingolipid and cholesterol synthesis for the barrier, little is known about the expression and regulation of the enzymes of phospholipid synthesis in the epidermis. In mammals, the glycerol-3-phosphate pathway is responsible for the majority of de novo glycerolipid biosynthesis (9–11). Glycerol-3-phosphate acyltransferase (GPAT; E.C.2.3.1.15) catalyzes the initial step in glycerolipid synthesis and is likely to play a critical regulatory role in glycerolipid synthesis (9–11). In mammalian cells, GPAT activity exists in multiple enzymatic isoforms that differ in subcellular localization, sensitivity to N-ethylmaleimide (NEM) inactivation, and substrate preferences (9–11). To date, four GPAT genes (GPAT1, 2, 3, and 4) have been cloned and their products demonstrated to have GPAT activities. GPAT1 encodes a NEM-resistant enzyme, which is located in the outer membrane of mitochondria with a substrate preference for saturated palmitoyl-CoA. GPAT2 encodes a NEM-sensitive mitochondrial isoform, but it is expressed less widely and to date it has been found only in testis and liver. Both GPAT3 and GPAT4 are endoplasmic reticulum (ER)-associated, NEM-sensitive enzymes, and appear to utilize a broad range of long-chain fatty acyl-CoAs, including both saturated and unsaturated species, as their substrate (9–11).

The regulation of GPAT expression is not well understood. The expression of GPAT1 in liver and adipose tissue decreases with fasting and increases with feeding (12–14). Additionally, insulin stimulates GPAT1 expression by increasing the activity of the transcription factor sterol-regulatory element binding protein (SREBP)-1 (15–17). Similarly, liver X receptor (LXR) activation also increases GPAT1 expression by increasing SREBP-1 activity (16). Furthermore, adipocyte differentiation increases both GPAT-1 and -3 mRNA levels and activation of peroxisome proliferator-activated receptor (PPAR)γ increases GPAT3 expression (18–20).

Given the critical role of GPATs in phospholipid and triglyceride biosynthesis, in this study, we first determined which GPAT isoforms are expressed in the epidermis/keratinocytes and second, how GPAT expression is regulated in epidermis/keratinocytes.

MATERIALS AND METHODS

Materials

22(R)-OH-cholesterol (22R), WY14643 (WY), *all-trans* retinoic acid (AT), and 9-*cis*-retinoic acid (9-*cis*) were purchased from Sigma (St Louis, MO). Ciglitazone (Cig) and troglitazone (Tro) were purchased from Cayman Chemical Co. (Ann Arbor, MI). Synthetic PPAR-δ activator GW610742× (GW) was a generous gift from Dr. Tim Willson (GlaxoSmithKline). 1*a*, 25-Dihydroxyvitamin D3 (VitD3) was purchased from BIOMOL International (Plymouth Meeting, PA). Molecular grade chemicals such as TRI Reagent were obtained from either Sigma or Fisher Scientific (Fairlawn, NJ). The iScript™ cDNA Synthesis Kit for first-strand cDNA synthesis was purchased from Bio-Rad Laboratories (Her-

cules, CA). All reagents and supplies for real-time PCR were purchased from Applied Biosystems (Foster City, CA).

Epidermis preparation

Timed pregnant Sprague-Dawley rats (plug date = day 0), estimated gestational age days 17–22, were obtained from Simonsen Laboratories (Gilroy, CA). Whole skin from each estimated gestational age group of fetal rats was collected as described (21). The epidermis from adult mouse or fetal rat was isolated as described previously (21). For the fetal rat study, four samples were analyzed for each time point. For day 19, 20, 21, and 22 rats, epidermis was isolated from a single fetus for each sample. For day 17 and 18 rats, to obtain sufficient material for RNA analysis, epidermis was pooled from two to three fetuses for each data point. The upper [SC/stratum granulosum (SG)]/stratum spinosum (SS) and lower (stratum basale, SB) epidermal fractions were obtained by incubating epidermis from hairless mice in 10 mM DTT/PBS at 37°C, as previously described in detail (22).

Acute barrier disruption model

Female hairless mice (hl/hl), 8–12 weeks old, were purchased from Charles River Laboratories (Wilmington, MA). For acute barrier disruption model, adult female hairless mouse skin was treated either by sequential applications of cellophane tape or by gently applying acetone-soaked cotton balls for 5–10 min as described previously (23). Transepidermal water loss (TEWL) was measured immediately after treatment using a Meeco electrolytic water analyzer as described previously. Animals with a transepidermal water loss rate of $\geq$ 4 mg/cm^2/h (normal <0.3 mg/cm^2/h) after barrier disruption were included in the study.

Keratinocyte culture and treatment

Human foreskin keratinocytes were isolated by a modification of the method of Pittelkow and Scott under an Institutional Review Board approved protocol (University of California, San Francisco). The second passage of keratinocytes was seeded and maintained in 0.07 mM calcium chloride (Cascade Biologics, Portland, OR). Once the cells attached, the culture medium was switched to either low (0.03 mM) or high (1.2 mM) calcium conditions as described previously (24). Control keratinocytes were treated with vehicle ($\leq$ 0.05% ethanol or DMSO).

qPCR analysis

Quantitative real-time PCR (qPCR) was performed with a Stratagene Mx3000P as previously described (25). Briefly, following RNA isolation, cDNA was synthesized to measure the relative mRNA levels of GPAT isoforms. The primer sequences for PCR are listed in Table 1. The PCR reaction was performed in duplicate, with 3–5 samples in each group, and the expression levels of each gene were normalized against cyclophilin [for cultured human keratinocytes (CHKs)] or 36B4 (for fetal rat or mouse epidermis), as described previously (26). Experiments were repeated at least once using a different batch of cells to ensure reproducibility.

GPAT assay

Total membrane and microsomal fractions were prepared from human keratinocytes for GPAT assay using methods previously described with modification (18, 27). Briefly, following the treatment, cells were washed three times with ice-cold PBS, collected, and homogenized in sucrose buffer (0.25 M sucrose, 10 mM Tris-HCl, pH 7.4, 1 mM EDTA, protease inhibitor cocktail) in a Teflon-glass motor-driven homogenizer on ice (sample A). Sample A was then centrifuged (800 g, 10 min) to remove debris and nuclei, followed by 100, 000 g (1.5 h) to obtain total membrane fractions (sample B). For microsomal preparation, sample A was centrifuged

at 16, 000 g (10 min) to remove cell debris and mitochondria; supernatants were collected and further centrifuged at 100, 000 g (1.5 h) to obtain microsomal fraction (sample C). Protein concentration was determined by the bicinchoninic acid (BCA) method (Pierce). GPAT activities were measured in a mixture containing 75 mM Tris-HCl (pH 7.5), 4 mM MgCl$_2$, 1 mg/ml BSA (essentially fatty acid-free), 75 μM lauroyl-CoA, and 80 μM [^{14}C]glycerol-3-phosphate (150 mCi/mmol) (American Radiolabeled Chemicals, St. Louis, MO). The reaction was initiated in a volume of 200 μl by adding 20 μg sample protein to the assay mixture and incubated for 20 min at 23°C. For NEM-resistant GPAT activities, total membrane fractions (sample B) were incubated with 400 μM NEM at 40°C for 15 min prior to determination of the activities. At the end of 20 min incubation, lipids were extracted with chloroform/methanol (2:1, v/v), dried, and separated by TLC, and chromatographed in parallel with authentic lipid standards. The [^{14}C]labeled lipids were visualized following exposure to phosphoimager screen/X-ray film; spots corresponding to lysophosphatidic acid (LPA) were scraped into scintillation vials containing ScintSafe (Fisher) and counted.

Metabolic labeling studies

CHK cells in 6-well plates were treated with either vehicle or PPAR ligands for 24 h, followed by incubation with trace [1-^{14}C]oleic acid (28) for an additional 16 h in the presence or absence of ligands. At the end of incubation, cells were washed with cold PBS and total lipids were extracted with chloroform/methanol (2:1, v/v). Two sets of extraction were performed to collect the lower chloroform phase. Polar and nonpolar phospholipids were separated by TLC with two different solvent systems, chloroform: methanol:acetic acid:formic acid: water (35:15:6:2:1), and hexane:diethyl ether:water (70:34:1), respectively. All samples were chromatographed in parallel with authentic lipid standards. Triglyceride and phosphoslipid spots were identified by comparison to known standards after visualization with iodine vapor. The [^{14}C]labeled lipids were visualized following exposure to phosphoimage screen/X-ray film, and relative abundance was quantified using the Quantity One system (Bio-Rad).

mRNA stability

Human keratinocytes were grown in low calcium medium until 60% confluency, and then incubated with the medium containing 5μM Cig or vehicle alone (ethanol) for 24 h. Cells were then treated with 2μg/ml actinomycin D for indicated periods of time (0, 3, 6, 16, and 24 hrs), harvested at each time point, and subjected to RT-QPCR analysis for determining hGPAT3 mRNA levels. The interpolation, calculation, and graphing of mRNA values were performed using SigmaPlot 8.0 software (Systat Software, Inc., Point Richmond, CA).

Construction of GPAT3 promoter-luciferase reporter genes

The 3210-bp human GPAT3 promoter was obtained by amplifying human Hep3B cell genomic DNA with primers (Table 1). This 3210-bp fragment was then cloned into pCR4 TOPO (Invitrogen) and followed by subcloning into pGL3.1 (Promega, Madison, WI). An additional 5′-terminal deletion variant (1061-bp) was generated by subcloning into the multicloning site of pGL3 basic with similar approaches. The final construct was sequenced to ascertain the orientation and fidelity of promoter sequence.

Transient transfections and reporter gene assay

CHK cells were seeded on 6-well plates at a density of 2×10^5/well to yield a confluence of 40–50% on the day of transfection. In a typical experiment, 1μg promoter-driven luciferase construct and 0.2 μg RSV-β-gal (a reporter plasmid), with Fugene 6 reagent (Roche) were added in media following the manufacturer's instruction. After incubation for 5 h at 37°C, transfection medium was removed and cells were washed once, followed by incubation in basal medium for additional 16 h. Cells were then treated with either vehicle or ligands for 24 or 48 h as indicated. At the end of the treatment, cells were rinsed and harvested for determining the luciferase activity, following the manufacturer's instructions (Promega, Madison, WI). β-Galactosidase activity was used to normalize transfection efficiencies.

Statistical analysis

The results are presented as means ± SEM, using Student's t-test for comparison between two groups. Comparisons within multiple groups were subjected to one-way ANOVA test, followed by Dunnett's posthoc test to analyze the variance between two groups. A P-value < 0.05 was considered significant.

RESULTS

Expression of GPAT isoforms in epidermis and cultured human keratinocytes

In mammals, GPAT exists in at least four isoforms. Our initial studies focused on determining which isoforms are expressed in mouse epidermis and cultured human keratinocytes. Specific primers for each isoform were designed (**Table 1**) and subsequently tested to ensure successful amplification of each GPAT isoform by our RT-qPCR protocol. Using total RNA isolated from mouse adult epidermis,

TABLE 1. Primers used in this study

Gene	Forward	Reverse	
hGPAT1	AACCCCAGTATCCCGTCTTT	CAGTCACATTGGTGGCAAAC	qPCR
hGPAT2	GGCTGACGGAGGAGATACTG	AGTTGTGCCAGGTGTGTGAG	qPCR
hGPAT3	ACAGCAGCCTCAAAAACTGG	CAATGGGGGAAGTATGGTTG	qPCR
hGPAT4	TGCCAAATGGGAGGTTTAAG	GCCACCATTTCTTGGTCTGT	qPCR
mGPAT1	CAACACCATCCCCGACATC	GTGACCTTCGATTATGCGATCA	qPCR
m/rGPAT2	CTCCTGGTTGCAGAGGAGA	AGCAGCTTTGCACTCAGATG	qPCR
m/rGPAT3	GGAGGATGAAGTGACCCAGA	CCAGTTTTTGAGGCTGCTGT	qPCR
mGPAT4	TGTCTGGTTTGAGCGTTCTG	TTCTGGGAAGATGAGGATGG	qPCR
rGPAT1	GTCCAAAGCCATCCAGAAAG	GAAACAAGAGCGGCAGATTC	qPCR
rGPAT4	ATGTTCCTGTTGCTGCCTTT	GGTTCTTCTCCTTGGCTCCT	qPCR
mr36B4	GCGACCTGGAAGTCCAACTAC	ATCTGCTGCATCTGCTTGG	qPCR
hCyclo	TCTCCTTTGAGCTGTTTGCAG	CACCACATGCTTGCCATC	qPCR
mAQP3	GACAGAAGGAGCTGGTGTCC	ATGAGGATGCCCAGAGTGAC	qPCR
mABCA12	ACAGGAATGGCCTTCATCAC	AACATGGTGCCCTGAGAAAC	qPCR
GPAT3-p3210	AGTCGGTACCGCTGCCACAAACCAAAGAAT (upper)		Reporter
	GACGCTCGAGGCGACCACTGACCTTGAGA (lower)		
GPAT3-p1061	GCTCTGCGTTTTCCTGTCC (upper)		Reporter

GPAT isoform 1, 3, and 4 were specifically amplified with C_T values of ~24-25 for GPAT1, ~23-24 for GPAT3, and ~27-28 for GPAT4. Under the same experimental condition, GPAT2 mRNA was not detected, suggesting that GPAT2 is not expressed in mouse epidermis. However, using the same primers we were able to detect GPAT2 mRNA in mouse liver (data not shown). As shown in **Table 2**, GPAT1, 3, and 4 are all relatively abundantly expressed in mouse epidermis, fetal rat epidermis, and CHKs but the relative expression levels vary. Again, GPAT2 is not expressed. Thus, three GPAT isoforms are expressed in epidermis/keratinocytes.

To determine the localization of GPAT1, 3, and 4 in intact mouse epidermis, upper (SC/SG/SS) and lower epidermal (SB) fractions were isolated using DTT, as reported previously (22, 29). To verify the purity of our epidermal preparations, we first measured the mRNA levels of two marker genes, ABCA12 (highly expressed in the upper epidermis) and aquaporin 3 (highly expressed in the basal layer). Using our experimental protocol, ABCA12 was found mainly in the upper epidermis whereas aquaporin 3 was found predominantly in the lower epidermis (**Fig. 1A**). Using this method, we demonstrated that although microsomal GPAT-3 and -4 are mainly localized to the upper epidermis, the mitochondrial isoform GPAT1 is found in both upper and lower epidermis (Fig. 1B).

The expression of GPAT isoforms during fetal rat epidermal development

In the fetal rat, epidermal stratification begins on day 17 and a multilayered SC with a competent barrier to transepidermal water loss is formed between day 19 and 21 (30). Pups are born with a mature fully developed SC on day 22. To determine the expression of GPAT during epidermal development, fetal epidermis was collected from 17 to 22 day pups and GPAT mRNA levels were determined by RT-qPCR. As shown in **Fig. 2**, the mRNA levels of GPAT1 and GPAT3 increased on day 19, reaching a peak on day 20, and declining thereafter. MRNA levels of GPAT4 showed lesser changes with a small increase (24%, $P < 0.05$) on day 20. These results indicate that the expression of GPAT1 and GPAT3 increases during fetal epidermal development concurrent with the formation of lamellar bodies and SC extracellular lipid membranes (30). In contrast, the expression GPAT1, 3, or 4 did not change following acute barrier disruption in hairless mouse epidermis (data not shown), indicating that basal

TABLE 2. C_T values of GPAT isoforms in mouse epidermis, CHKs, or rat epidermis

GPAT Isoforms	Mouse Epidermis	CHKs	Rat Epidermis
	(Adult)		(Fetal)
GPAT1	24 ~25	25 ~27	22 ~24
GPAT2	nd	nd	nd
GPAT3	23 ~24	30 ~32	24 ~27
GPAT4	27 ~28	27 ~28	23 ~24

C_T values are inversely proportional to the amount of target mRNA in the sample (ie., the lower the C_T level the greater the amount of mRNA in the sample). $C_T \leq 29$ indicate abundant target mRNA in the sample. nd, not detected.
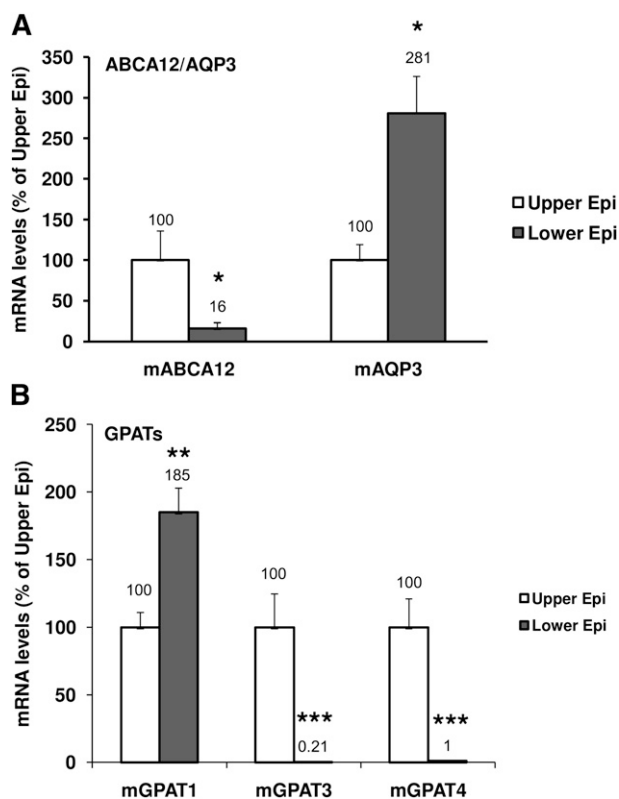
Fig. 1. Localization of GPAT in the epidermis of mice. The upper and lower epidermis was prepared as described in Materials and Methods, and the relative mRNA expression levels of marker genes (ABCA12, aquaporin 3) (A) and GPAT isoforms (GPAT-1, -3, -4) (B) were determined. Results are expressed as a percentage of the upper epidermis (100%) and presented as mean ± SEM (n = 6). The experiment was repeated once using a different batch of mice with similar results. *$P < 0.05$, **$P < 0.01$, ***$P < 0.001$.

GPAT expression suffices to meet permeability barrier requirements in adult mice.

Differential regulation of GPAT isoforms during keratinocyte differentiation

We next determined whether the expression of GPAT isoforms is regulated during keratinocyte differentation. Keratinocytes cultured in low levels of extracellular calcium (0.03 mM) remain in a proliferative state, whereas a high calcium media (e.g., 1.2 mM) is well known to stimulate keratinocyte differentiation (31, 32). Therefore, we next determined whether the expression of GPAT isoforms changes in CHKs after switching to high calcium conditions (**Fig. 3A**). To confirm that differentiation was induced under these conditions, the mRNA levels of an early differentiation marker, involucrin, increased within 24 h (33), and this increase was sustained at a high level through day 7 (data not shown). Under the same experimental conditions, GPAT3 mRNA levels exhibited a very modest early increase (~40–50% increase on day 1–3) with a more robust increase with longer incubation (3- and 7-fold increase at day 4 and 7, respectively). In contrast, GPAT1 and GPAT4 mRNA levels did not increase, but rather decreased by ~50% at most time points during keratinocyte differentiation (Fig. 3A). Taken together, these
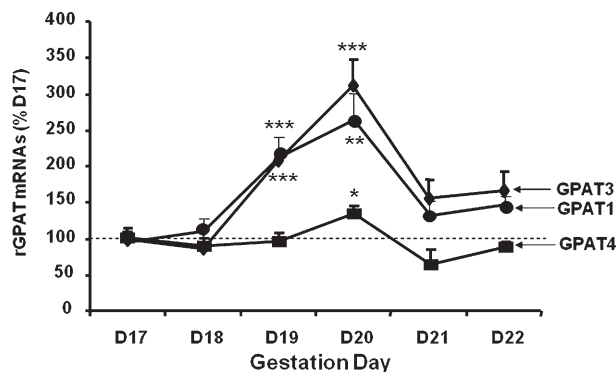
Fig. 2. MRNA levels of GPATs in fetal rat epidermis during late gestation. Fetal rat epidermis was prepared as described in Materials and Methods. Total RNA was extracted for RT-qPCR analysis. The relative mRNA expression levels of GPAT isoforms (GPAT-1, -3, -4) are shown. Data are expressed as a percentage of day 17 (as control) and presented as mean ± SEM (n = 4). Note that each sample for day 17 and 18 are pooled epidermis isolated from 2 to 3 fetal rats. *$P < 0.05$, **$P < 0.01$, ***$P < 0.001$.

studies demonstrate that GPAT isoforms are differentially regulated during keratinocyte differentiation with GPAT3 expression increasing.

To begin to ascertain the functional effects of alterations in GPAT expression during differentiation, we next measured GPAT activity in calcium-differentiated CHKs versus undifferentiated controls. As shown in Fig. 3B, total GPAT activity approximately doubled in differentiated as compared with undifferentiated keratinocytes. GPAT3 encodes an NEM-sensitive enzyme and NEM-sensitive GPAT activity increased ∼3-fold. In contrast, NEM-resistent GPAT activity, a marker of GPAT1 activity, showed little change during keratinocyte differentiation. Finally, because GPAT3 localizes to the microsomal fraction, we next measured microsomal GPAT activity and, as shown in Fig. 3C, microsomal activity increased ∼8-fold during calcium-induced keratinocyte differentiation. These results indicate that there is an increase in bulk GPAT activity in human keratinocytes during differentiation, and that this increase in activity corresponds with an increase in GPAT3 mRNA levels and increased NEM-sensitive activity that localizes to microsomes.

Activators of PPARs/LXR stimulate GPAT3 expression in CHKs

Previously, we and others have demonstrated that PPARs and LXRs are expressed in human keratinocytes and their activators promote differentiation (34). Because activation of PPARγ and LXR has also been shown to increase GPAT1 and/or GPAT3 mRNAs in both mouse liver and in cultured 3T3-L1 adipocytes (16, 35), we next determined whether activation of PPARα, PPARδ, PPARγ, LXR, retinoid X receptor (RXR), retinoic acid receptor (RAR), or vitamin D receptor (VDR) alters GPAT mRNA levels. GPAT3 mRNA levels increase markedly following treatment with PPARγ activators (Cig: ∼5-fold, Tro: 2.8-fold) (**Fig. 4A**). Similarly, treatment of CHKs with other nuclear receptor activators also significantly increase GPAT3 mRNA level, but to a
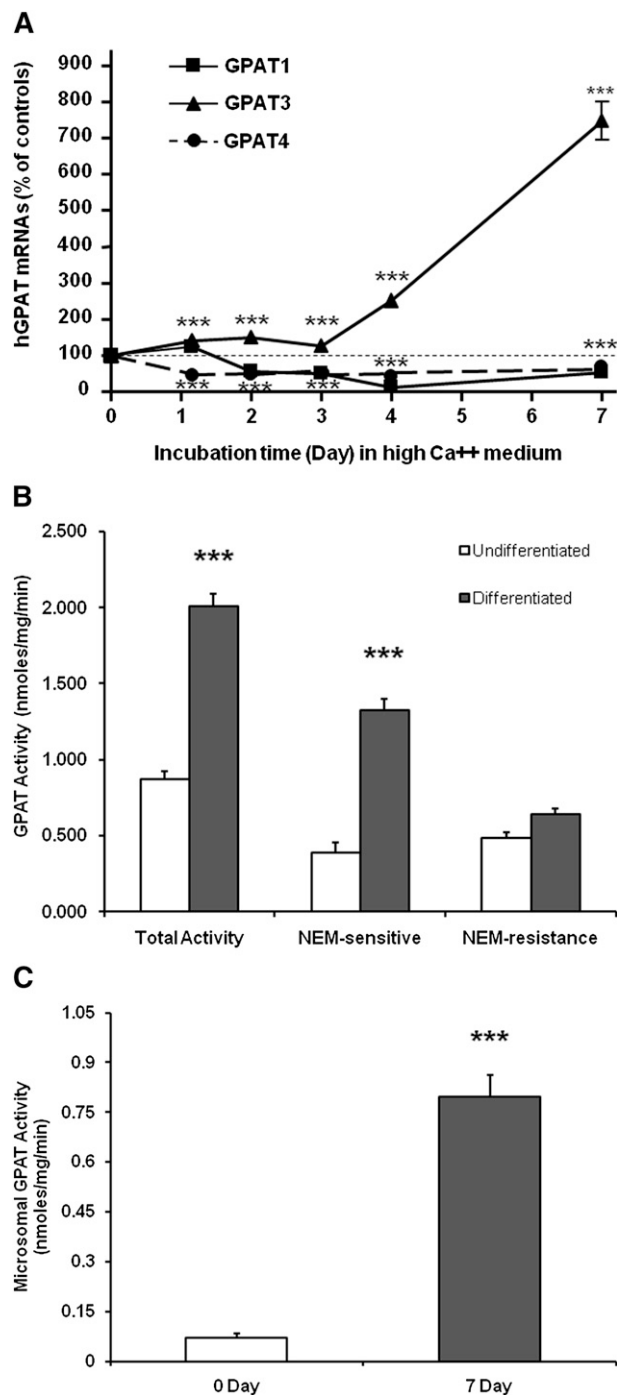
Fig. 3. Upregulation of GPAT3 gene expression during calcium-induced keratinocytes differentiation. CHK cells were incubated in high (1.2 mM) calcium medium for indicated periods of time (0, 1, 2, 3, 4, 7 days), and mRNA levels for GPAT isoforms were determined by RT-qPCR (A). Data are expressed as percentage of undifferentiated keratinocyte (day 0), and presented as mean ± SEM (n = 4). In a separate set of experiments (B), CHK cells were incubated in 1.2 mM calcium for 0 day or 7 days, and the total, NEM-sensitive, or NEM-resistant GPAT activities were determined. Alternatively, the microsomal GPAT activities were determined from a microsomal preparation (C). Data are presented as mean ± SEM (n = 3). ***$P < 0.001$.
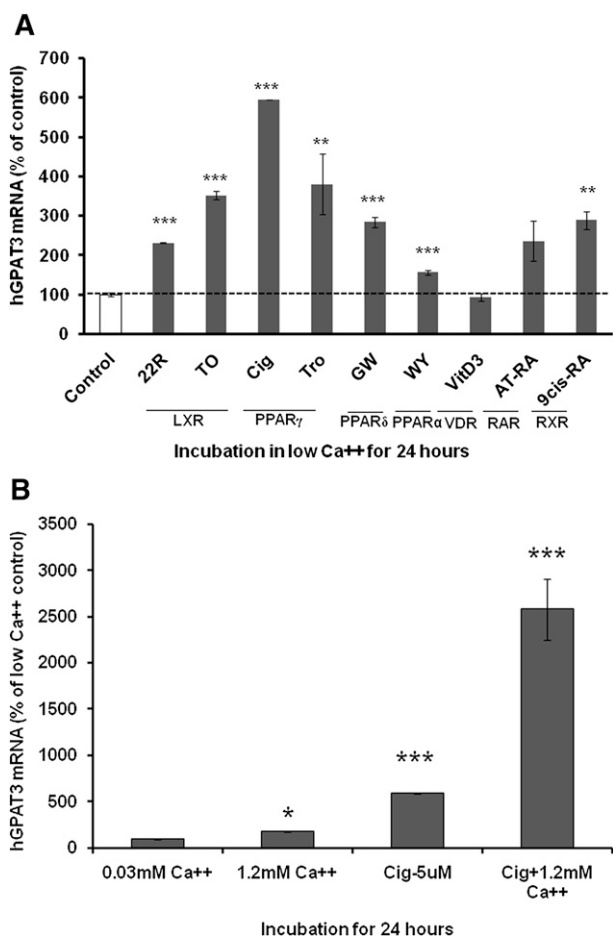
Fig. 4. Ligand activation of PPARs, LXR, or RXR stimulates GPAT3 gene expression in CHKs. Cells were incubated with either vehicle or activators of PPARα (WY, 20 µM), PPARδ (GW 610742×, 8 µM), PPARγ (Cig, 5 µM; Tro, 7.5 µM), LXR (22R, 10 µM; TO 901317, 10 µM), vitamin D receptor (VitD3, 0.1 µM), RAR (AT-RA, l µM), and RXR (9cis-RA, 1 µM) in low calcium medium for 24 h (A). Alternatively, cells were incubated with either low calcium alone, low calcium plus Cig (5 µM), high (1.2 mM) calcium alone, or high calcium plus Cig (5 µM) for 24 h (B). RT-qPCR was performed to measure mRNA levels of GPAT3. Data are expressed as percentage of vehicle control and presented as mean ± SEM (n = 5). **$P < 0.01$, ***$P < 0.001$. ATRA, *all*-trans retinoic acid; VitD3, 1, 25-dehydroxyvitamin D3.

lesser degree: PPARδ (GW: ∼1.8-fold); PPARα (WY: ∼60%); LXR (22R: ∼1.3-fold, TO: 2.5-fold); and RXR (9-*cis*: ∼1.9-fold). In contrast, 1, 25 dihydroxy vitamin D3 had no effect on GPAT3 mRNA levels despite its well recognized ability to induce keratinocyte differentiation. The absence of an effect of 1, 25 dihydroxy vitamin D3 is likely due to the short duration of our experiments, as previous studies have shown that 1, 25 dihydroxy vitamin D3 requires ⩾ 30 h to induce the expression of involucrin and transglutaminase I, classic differentiation markers (33). Finally, under the same experimental condition, neither GPAT1 nor GPAT4 mRNA levels were significantly modulated by activation of these nuclear receptors (data not shown), suggesting specific regulation of GPAT3 expression in CHKs.

We next determined the effect of the PPARγ activator Cig in a high Ca^{2+} (1.2 mM) medium. As shown in Fig. 4B,

the combination of Cig and high Ca^{2+} resulted in a synergistic increase in GPAT3 mRNA levels.

The PPARγ activator-induced increase in GPAT3 gene expression appears to be both time- and dose-dependent. The Cig-induced increase in GPAT3 mRNA level occurs as early as 4 h, peaks at 16 h, and declines at later times in CHKs (**Fig. 5A**). Furthermore, treatment with Cig also resulted in a dose-dependent increase in GPAT3 mRNA levels, with a maximal ∼6-fold increase at 7.5 µM. (Fig. 5B). Although activation of PPARδ by GW also causes a time- (Fig. 5C) and dose-dependent induction of GPAT3 mRNA (Fig. 5D), the increase is delayed compared with PPARγ activation (Fig. 5A). Finally, to investigate whether the Cig-induced increase in GPAT3 mRNA levels in CHKs is associated with changes in microsomal GPAT (mGPAT) activity, we next examined mGPAT activity in the presence or absence of Cig. Treatment of CHKs with Cig causes a significant increase in mGPAT activity by ∼3-fold (**Fig. 6A**).

We next determined the effect of Cig treatment on glycerolipid biosynthesis in CHK. Following Cig or vehicle treatment for 24 h, cells were incubated with $[1-^{14}C]$oleic acid to examine the incorporation into triglyceride and phospholipids. As expected, Cig significantly increases $[1-^{14}C]$ oleate incorporation into triglyceride (∼90%), PC (∼20%), and lysoPC (∼20%) as compared with vehicle controls (Fig. 6B). In contrast, Cig treatment did not alter incorporation into PE/PS (Fig. 6B). Together, these results indicate that activation of nuclear receptors, in particular PPARγ, stimulates GPAT3 gene expression, leading to both enhanced microsomal GPAT activity and increased glycerolipid synthesis in CHKs. Whether the increase in glycerolipid synthesis is solely due to an increase in GPAT activity or whether other enzymes in the synthetic pathway also are induced by PPARγ activators remains to be determined. Of note, we did not observe any significant effects of PPAR-α, -δ, -γ, or LXR activators on the mRNA levels of AGPAT-1, -2, -3, -4, and -5 expression in CHKs (data not shown), suggesting that increases in the activity of this enzyme are not likely to be responsible for the increase in glycerolipid synthesis.

Activation of PPARs transactivates GPAT3 gene expression

The upregulation of GPAT3 mRNA could result from either increased gene transcription and/or decreased degradation (stability). To distinguish among these possibilities, we first examined the effect of Cig on GPAT3 mRNA stability. As shown in **Fig. 7A**, Cig treatment does not significantly alter GPAT3 mRNA stability in CHKs (half-life ∼13 h) compared with vehicle control (∼15 h). We next determined the response of the promoter region of GPAT3 to Cig or GW in human GPAT3 promoter constructs (1061-bp) linked to a luciferase reporter gene. Following the transient transfection of CHKs with this construct, luciferase activity was determined, and the luciferase activity of the 1061-bp GPAT3 promoter increased significantly (∼2.3-fold and ∼91%) with Cig and GW treatment, respectively (Fig. 7B). Moreover, another PPARγ ligand, Tro, also increased luciferase
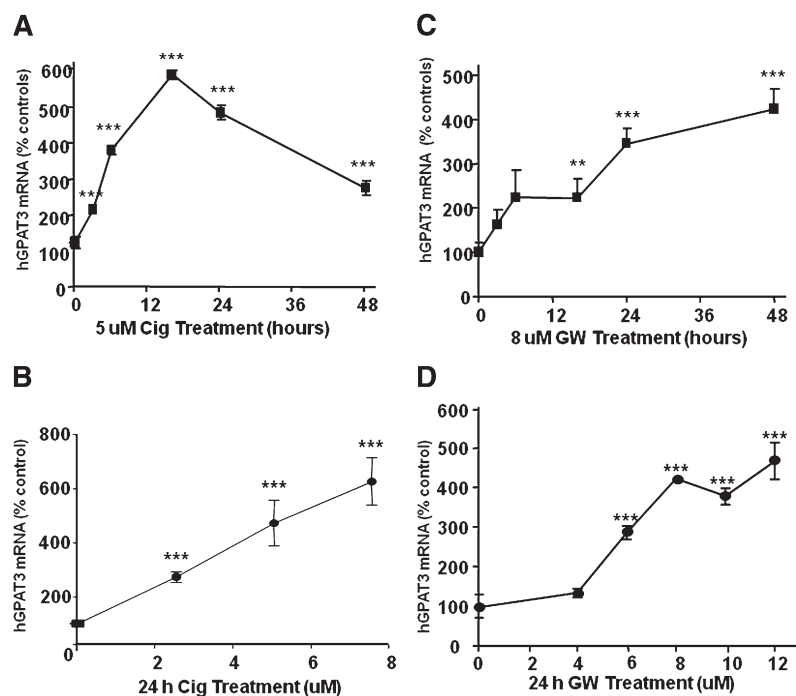
Fig. 5. Ligand activation of either PPAR-γ or PPAR–δ increases GPAT3 mRNA levels in a dose-and time-dependent fashion in CHKs. Cells were incubated with various concentrations of either Cig (0, 2.5, 5, 7.5 µM) (A), GW 610742× (0, 4, 6, 8, 10, 12 µM) (C), or vehicle in low calcium medium for 24 h. Alternatively, cells were incubated with either Cig (5 µM) (B) or GW 610742× (8 µM) (D) for various periods of time (0, 3, 6, 16, 24, and 48 h) in low calcium medium. GPAT3 mRNA levels were determined by RT-qPCR. Data are expressed as percentage of control and presented as mean ± SEM (n = 3). For the time course studies, data are presented as percentage of vehicle control (in the absence of GW 610742× or Cig) for each matched time point. **$P < 0.01$, ***$P < 0.001$.

activity (data not shown). The Cig- or GW-induced increase in luciferase activity paralleled a comparable increase in GPAT3 mRNA upon Cig or GW treatment under these transfection conditions (data not shown). Together, these data indicate that human GPAT3 gene expression is stimulated by PPARγ and PPARδ activation at the transcriptional level.

DISCUSSION

The formation of the stratum corneum requires the de novo synthesis of triglycerides and phospholipids (1). The triglycerides likely play an important storage role, with the breakdown of triglycerides providing fatty acids for phospholipid and ceramide synthesis. Genetic disorders that prevent the breakdown of triglycerides in the epidermis, such as neutral lipid storage disease (Chanarin-Dorfman syndrome), result in severe abnormalities in permeability barrier function (36, 37). Recently, mice deficient in comparative gene identification -58 (CGI-58), a lipid droplet associated protein that facilitates triglyceride hydrolysis, have been shown to develop a severe permability barrier defect due to the impaired hydrolysis of epidermal triglyceride and decreased formation of acyl ceramides (38). The newly synthesized phospholipids, along with glycosphingolipids and cholesterol, are assembled into lamellar bodies and subsequently secreted into the extracellular spaces of the SC, where they mediate permeability barrier function (1). Given the critical role of triglycerides and phospholipids in permeability barrier function, it is important to characterize the enzymes involved in triglyceride and phospholipid synthesis in the epidermis and their regulation. GPAT catalyzes the formation of lysophosphatidic acid, the first step in the formation of triglycerides and phospholipids (9–11).
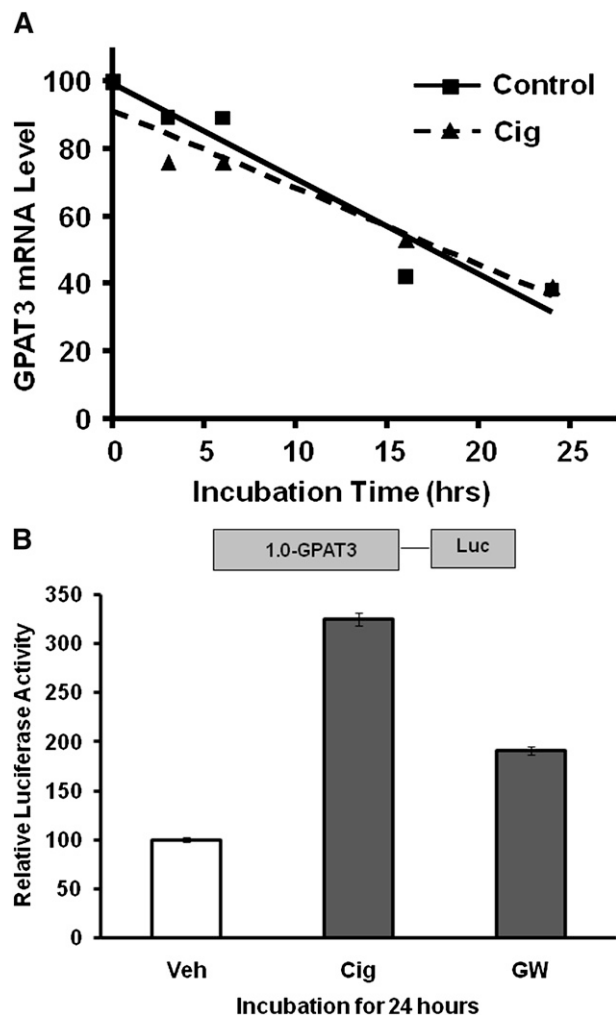
In this study, we demonstrate that three different GPAT isoforms are expressed in the epidermis/keratinocytes. GPAT 3 and 4 are expressed predominately in the upper epidermal layers whereas GPAT 1 is expressed in both the upper and lower epidermal layers of the mouse. Based on mRNA levels, GPAT1, 3, and 4 are all expressed at relatively high levels (Table 2). GPAT2 is not detected in either keratinocytes or the epidermis but it is detected in the liver. In CHKs, C_T values of ∼25-27 for GPAT1, ∼30-32 for GPAT3, and ∼27-28 for GPAT4 were observed. These results correspond with the observation that approximately one-half of GPAT activity in keratinocytes is NEM sensitive, which could represent either GPAT3 or GPAT4, while one-half of GPAT activity is NEM resistant, which could represent GPAT1 activity. The distribution of GPAT isoforms varies greatly from tissue to tissue. In the liver, mitochondrial GPAT1 accounts for 50% of GPAT activity (39, 40) whereas in heart, white adipose tissue, and brown adipose tissue, microsomal GPAT activity (GPAT 3 and 4) accounts for most of the activity (9, 10, 41, 42). In contrast, in skeletal muscle, greater than 90% of GPAT activity is accounted for by GPAT1 (43). In CHKs, ∼50% of total GPAT activity appears to be accounted for by GPAT1 (NEM resistant) and 50% by GPAT 3 and 4 (NEM sensitive) (this study).

To determine the functional role of the GPAT isoforms, we assessed changes in expression and activity in relation to epidermal development in utero, keratinocyte differentiation, and after barrier disruption. During fetal epidermal development, the expression of both GPAT1 and GPAT3 increase 2- to 4-fold between day 17 and 20, a period during which a mature epidermis with a functional permeability barrier is formed (30). The expression of GPAT4 shows little change during fetal epidermal development. One can speculate that the increase in GPAT1 and GPAT3 provides an increased supply of triglycerides
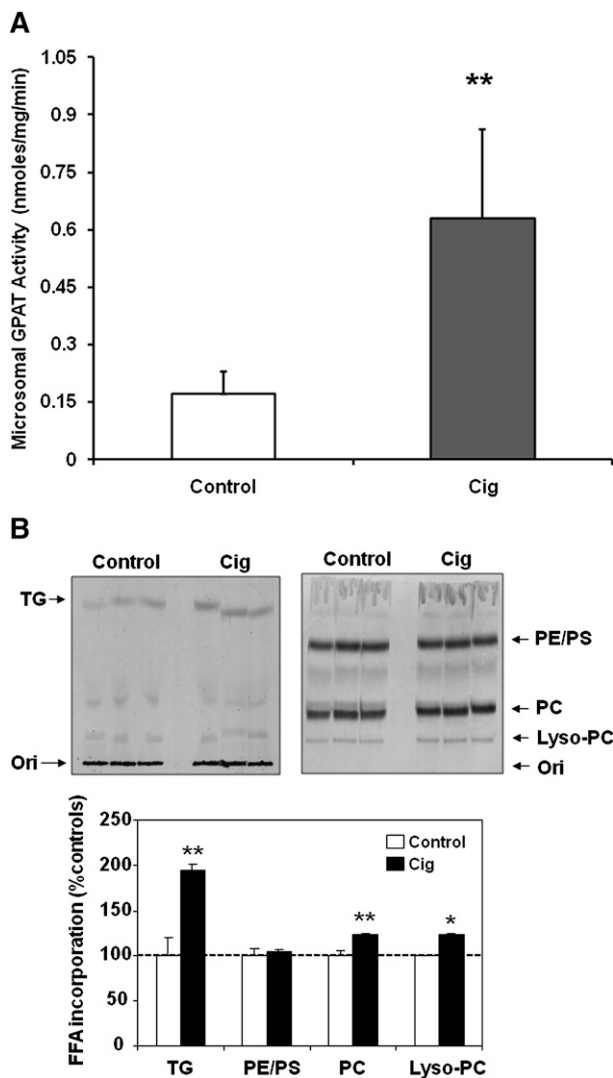
Fig. 6. Ligand activation of PPAR-γ increases microsomal GPAT3 activity and the incorporation of [1-^{14}C] oleic acid into glycerolipids in CHKs. Cells were incubated with either vehicle or Cig (7.5 µM) in low calcium medium for 24 h, and the microsomal GPAT activities were measured as described in Materials and Methods (A). In a separate set of experiments, following Cig or vehicle treatment, cells were incubated with trace [1-^{14}C]oleic acid for an additional 16 h in the presence or absence of Cig (B). Total lipids and the relative incorporation of [1-^{14}C] oleic acid into TG or phospholipids were analyzed as described and expressed as percentage of vehicle control. Data are presented as mean ± SEM (n = 3). *P < 0.05, **P < 0.01.

Fig. 7. Ligand activation of PPARγ transactivates GPAT3 gene expression. A: CHK cells were incubated with either Cig (5 µM) or vehicle for 24 h and subsequently treated with 2 µg/ml of actinomycin D for the indicated periods of time (0, 3, 6, 16, and 24 h). GPAT3 mRNA levels were determined by RT-qPCR. Data are expressed as percentage of 0 h and presented as mean ± SEM (n = 3). B: Luciferase reporter plasmid containing human GPAT3 promoter was transfected into CHKs, followed by incubation with either vehicle, Cig (5 µM), or GW 610742× (8 µM) for 24 h in low calcium medium. Luciferase activity was determined relative to β-galactosidase. Data are presented as mean ± SEM (n = 3). **P < 0.01, ***P < 0.001.

and phospholipids that enable keratinocytes to synthesize lamellar bodies and secrete lipids to form a functional SC for a protective barrier. Previous studies on DGAT (acyl-CoA: diacylglycerol acyltransferase), a downstream enzyme that catalyzes TG synthesis from diacylglycerol and active fatty acyl-CoAs, have shown that DGAT2 but not DGAT1 is expressed in the epidermis, and that DGAT2 knockout mice die at birth at least in part due to the failure to form a mature epidermis that provides a barrier to water loss (44). In the current study, we do not observe a change in the expression of any GPAT isoform following acute barrier disruption (data not shown). Investigators have cre-

ated GPAT1 and GPAT4 knockout mice but cutaneous abnormalities have not been reported in these animals (45, 46), suggesting that neither GPAT1 nor GPAT4 is essential for the formation of a competent SC. To the best of our knowledge, GPAT3 knockout mice have not yet been described. Thus, determination of the role and importance of the various GPAT isoforms in the formation of the lipids required for the extracellular lipid membranes in the SC that provide the barrier to water loss will require further investigation.

During keratinocyte differentiation, the expression of a large number of genes is regulated. In the present study we demonstrate that the expression of GPAT3 increases as much as 7-fold during calcium-keratinocyte differentia-

tion, in contrast to a decrease in both GPAT1 and GPAT4 expression. Total GPAT activity increases ∼2-fold during keratinocyte differentiation, and this increase is entirely accounted for by an increase in NEM-sensitive GPAT activity with little change in NEM-resistant activity. In differentiated keratinocytes, NEM-sensitive GPAT activity accounts for about two-thirds of the total GPAT activity. Additionally, microsomal GPAT activity markedly increases during differentiation. Taken together, these results indicate that keratinocyte differentiation leads to an increase in GPAT activity that is most likely due to the increased expression of GPAT3. These results are analogous to previous reports demonstrating that GPAT3 expression increases dramatically during the differentiation of 3T3-L1 adipocytes (20, 47). It should be noted that although studies in CHKs do not demonstrate an increase in GPAT4 expression with differentiation, studies in mouse epidermis indicate that the expression of GPAT4 increases with differentiation. The explanation for the differences between the in vitro studies with CHKs and the in vivo studies with mouse epidermis remain to be elucidated but could be due to species differences or to limitations of in vitro models.

When diabetic mice are treated with PPARγ agonist, GPAT3 expression markedly increases in white adipose tissue (20). Similarly, here we show that in keratinocytes PPARγ activators also increase GPAT3 expression. The increase in GPAT3 expression is associated with almost a doubling in the synthesis of triglyceride with a smaller increase in phospholipid synthesis. In addition, PPARδ and LXR activators also increase GPAT3 expression. In contrast, PPARγ, PPARδ, and LXR activators do not affect the expression of either GPAT1 or GPAT4 in human keratinocytes. The increase in GPAT3 mRNA levels induced by PPARγ or PPARδ activators is due to an increase in gene transcription with limited change in RNA stability.

The results observed in the present study can be compared with our previous studies of 1-acyl-sn-glycerol-3-phosphate acyltransferases (AGPATs), the enzymes that catalyze the acylation of lysophosphatidic acid to form phosphatidic acid, the second step in the formation of triglycerides and phospholipids. We recently reported that AGPAT 3, 4, and 5 have relatively high constitutive expression in the epidermis with AGPAT1 and 2 having low constitutive expression (48). Moreover, acute permeability barrier disruption by either tape stripping or acetone treatment stimulates the expression of AGPAT1, 2, and 3 and is associated with an increase in AGPAT activity (48). Notably, this increase in AGPAT expression following barrier disruption can be blocked by artificially providing a permeability barrier, indicating that this increase is specifically related to alterations in permeability barrier function and is not simply due to nonspecific injury to the skin (48). Thus, similar to AGPAT, multiple isoforms of GPAT are expressed in the skin. However, in contrast to AGPAT, GPAT expression in the epidermis is not regulated by permeability barrier function. Furthermore, although all AGPAT isoforms (AGPAT1–5) are expressed in human keratinocytes, none of them are regulated by activators of either PPARs or LXR (unpublished observations).

One can only speculate on why multiple isoforms of GPAT and AGPAT are expressed in the epidermis. Clearly, the presence of multiple enzymes carrying out redundant enzymatic functions may allow for the epidermis to compensate for defects in one isoform. More likely, however, given the marked changes in structure and function that occur during keratinocyte differentiation, different isoforms may be needed at different stages of keratinocyte differentiation. In support of this notion, there is a marked increase in GPAT3 expression during keratinocyte differentiation. It is also possible, given the different fatty acid substrate preferences of the GPAT isoforms, that the synthesis of specific triglyceride and phospholipid species may be catalyzed by different GPAT isoforms. Finally, it is notable that the subcellular localization of the GPATs varies (9, 11), and it may be that different isoforms are required depending on fatty acid flux. For example, the breakdown of triglyceride may deliver fatty acids to the mitochondria where GPAT1 is located, whereas the de novo synthesis of fatty acids may deliver fatty acids to the microsomes where GPAT3 and 4 are located. It is apparent that the synthesis of triglycerides and phospholipids in the epidermis is mediated by numerous enzymes, suggesting that this process needs to be finely tuned to meet the requirements of the cell. The precise function of each GPAT isoform in the epidermis/keratinocytes will require further investigations.▪

REFERENCES

1. Feingold, K. R. 2007. Thematic review series: skin lipids. The role of epidermal lipids in cutaneous permeability barrier homeostasis. *J. Lipid Res.* **48:** 2531–2546.
2. Grayson, S., A. G. Johnson-Winegar, B. U. Wintroub, R. R. Isseroff, E. H. Epstein, Jr., and P. M. Elias. 1985. Lamellar body-enriched fractions from neonatal mice: preparative techniques and partial characterization. *J. Invest. Dermatol.* **85:** 289–294.
3. Schurer, N. Y., and P. M. Elias. 1991. The biochemistry and function of stratum corneum lipids. *Adv. Lipid Res.* **24:** 27–56.
4. Holleran, W. M., Y. Takagi, and Y. Uchida. 2006. Epidermal sphingolipids: metabolism, function, and roles in skin disorders. *FEBS Lett.* **580:** 5456–5466.
5. Elias, P. M., and K. R. Feingold, editor. 2006. Permability Barrier Homeostasis. Taylor & Francis, New York.
6. Mao-Qiang, M., P. M. Elias, and K. R. Feingold. 1993. Fatty acids are required for epidermal permeability barrier function. *J. Clin. Invest.* **92:** 791–798.
7. Feingold, K. R., M. Q. Man, G. K. Menon, S. S. Cho, B. E. Brown, and P. M. Elias. 1990. Cholesterol synthesis is required for cutaneous barrier function in mice. *J. Clin. Invest.* **86:** 1738–1745.
8. Holleran, W. M., M. Q. Man, W. N. Gao, G. K. Menon, P. M. Elias, and K. R. Feingold. 1991. Sphingolipids are required for mammalian epidermal barrier function. Inhibition of sphingolipid synthesis delays barrier recovery after acute perturbation. *J. Clin. Invest.* **88:** 1338–1345.
9. Wendel, A. A., T. M. Lewin, and R. A. Coleman. 2009. Glycerol-3-phosphate acyltransferases: rate limiting enzymes of triacylglycerol biosynthesis. *Biochim. Biophys. Acta.* **1791:** 501–506.
10. Takeuchi, K., and K. Reue. 2009. Biochemistry, physiology, and genetics of GPAT, AGPAT, and lipin enzymes in triglyceride synthesis. *Am. J. Physiol.* **296:** E1195–E1209.
11. Gimeno, R. E., and J. Cao. 2008. Thematic review series: glycerolipids. Mammalian glycerol-3-phosphate acyltransferases: new genes for an old activity. *J. Lipid Res.* **49:** 2079–2088.
12. Lewin, T. M., D. A. Granger, J. H. Kim, and R. A. Coleman. 2001. Regulation of mitochondrial sn-glycerol-3-phosphate acyltransferase activity: response to feeding status is unique in various rat tissues and is discordant with protein expression. *Arch. Biochem. Biophys.* **396:** 119–127.

13. Paulauskis, J. D., and H. S. Sul. 1988. Cloning and expression of mouse fatty acid synthase and other specific mRNAs. Developmental and hormonal regulation in 3T3–L1 cells. *J. Biol. Chem.* **263:** 7049–7054.

14. Shin, D. H., J. D. Paulauskis, N. Moustaid, and H. S. Sul. 1991. Transcriptional regulation of p90 with sequence homology to Escherichia coli glycerol-3-phosphate acyltransferase. *J. Biol. Chem.* **266:** 23834–23839.

15. Ericsson, J., S. M. Jackson, J. B. Kim, B. M. Spiegelman, and P. A. Edwards. 1997. Identification of glycerol-3-phosphate acyltransferase as an adipocyte determination and differentiation factor 1- and sterol regulatory element-binding protein-responsive gene. *J. Biol. Chem.* **272:** 7298–7305.

16. Liang, G., J. Yang, J. D. Horton, R. E. Hammer, J. L. Goldstein, and M. S. Brown. 2002. Diminished hepatic response to fasting/refeeding and liver X receptor agonists in mice with selective deficiency of sterol regulatory element-binding protein-1c. *J. Biol. Chem.* **277:** 9520–9528.

17. Shimano, H., N. Yahagi, M. Amemiya-Kudo, A. H. Hasty, J. Osuga, Y. Tamura, F. Shionoiri, Y. Iizuka, K. Ohashi, K. Harada, et al. 1999. Sterol regulatory element-binding protein-1 as a key transcription factor for nutritional induction of lipogenic enzyme genes. *J. Biol. Chem.* **274:** 35832–35839.

18. Coleman, R. A., and R. M. Bell. 1980. Selective changes in enzymes of the sn-glycerol 3-phosphate and dihydroxyacetone-phosphate pathways of triacylglycerol biosynthesis during differentiation of 3T3–L1 preadipocytes. *J. Biol. Chem.* **255:** 7681–7687.

19. Yet, S. F., S. Lee, Y. T. Hahm, and H. S. Sul. 1993. Expression and identification of p90 as the murine mitochondrial glycerol-3-phosphate acyltransferase. *Biochemistry.* **32:** 9486–9491.

20. Cao, J., J. L. Li, D. Li, J. F. Tobin, and R. E. Gimeno. 2006. Molecular identification of microsomal acyl-CoA:glycerol-3-phosphate acyltransferase, a key enzyme in de novo triacylglycerol synthesis. *Proc. Natl. Acad. Sci. USA.* **103:** 19695–19700.

21. Jiang, Y. J., B. Lu, D. Crumrine, M. Q. Man, P. M. Elias, and K. R. Feingold. 2009. IL-1alpha accelerates stratum corneum formation and improves permeability barrier homeostasis during murine fetal development. *J. Dermatol. Sci.* **54:** 88–98.

22. Feingold, K. R., B. E. Brown, S. R. Lear, A. H. Moser, and P. M. Elias. 1983. Localization of de novo sterologenesis in mammalian skin. *J. Invest. Dermatol.* **81:** 365–369.

23. Jackson, S. M., L. C. Wood, S. Lauer, J. M. Taylor, A. D. Cooper, P. M. Elias, and K. R. Feingold. 1992. Effect of cutaneous permeability barrier disruption on HMG-CoA reductase, LDL receptor, and apolipoprotein E mRNA levels in the epidermis of hairless mice. *J. Lipid Res.* **33:** 1307–1314.

24. Jiang, Y. J., B. Lu, P. Kim, G. Paragh, G. Schmitz, P. M. Elias, and K. R. Feingold. 2008. PPAR and LXR activators regulate ABCA12 expression in human keratinocytes. *J. Invest. Dermatol.* **128:** 104–109.

25. Jiang, Y. J., Y. Uchida, B. Lu, P. Kim, C. Mao, M. Akiyama, P. M. Elias, W. M. Holleran, C. Grunfeld, and K. R. Feingold. 2009. Ceramide stimulates ABCA12 expression via peroxisome proliferator-activated receptor {delta} in human keratinocytes. *J. Biol. Chem.* **284:** 18942–18952.

26. Jiang, Y. J., Y. Uchida, B. Lu, P. Kim, C. Mao, M. Akiyama, P. M. Elias, W. M. Holleran, C. Grunfeld, and K. R. Feingold. 2009. Ceramide stimulates ABCA12 expression via PPAR{delta} in human keratinocytes. *J Biol Chem.* **284:** 18942–18952.

27. Chen, Y. Q., M. S. Kuo, S. Li, H. H. Bui, D. A. Peake, P. E. Sanders, S. J. Thibodeaux, S. Chu, Y. W. Qian, Y. Zhao, et al. 2008. AGPAT6 is a novel microsomal glycerol-3-phosphate acyltransferase. *J. Biol. Chem.* **283:** 10048–10057.

28. Igal, R. A., S. Wang, M. Gonzalez-Baro, and R. A. Coleman. 2001. Mitochondrial glycerol phosphate acyltransferase directs the incorporation of exogenous fatty acids into triacylglycerol. *J. Biol. Chem.* **276:** 42205–42212.

29. Monger, D. J., M. L. Williams, K. R. Feingold, B. E. Brown, and P. M. Elias. 1988. Localization of sites of lipid biosynthesis in mammalian epidermis. *J. Lipid Res.* **29:** 603–612.

30. Aszterbaum, M., G. K. Menon, K. R. Feingold, and M. L. Williams. 1992. Ontogeny of the epidermal barrier to water loss in the rat: correlation of function with stratum corneum structure and lipid content. *Pediatr. Res.* **31:** 308–317.

31. Hennings, H., D. Michael, C. Cheng, P. Steinert, K. Holbrook, and S. H. Yuspa. 1980. Calcium regulation of growth and differentiation of mouse epidermal cells in culture. *Cell.* **19:** 245–254.

32. Bikle, D. D., and S. Pillai. 1993. Vitamin D, calcium, and epidermal differentiation. *Endocr. Rev.* **14:** 3–19.

33. Su, M. J., D. D. Bikle, M. L. Mancianti, and S. Pillai. 1994. 1,25-Dihydroxyvitamin D3 potentiates the keratinocyte response to calcium. *J. Biol. Chem.* **269:** 14723–14729.

34. Schmuth, M., Y. J. Jiang, S. Dubrac, P. M. Elias, and K. R. Feingold. 2008. Thematic review series: skin lipids. Peroxisome proliferator-activated receptors and liver X receptors in epidermal biology. *J. Lipid Res.* **49:** 499–509.

35. Way, J. M., W. W. Harrington, K. K. Brown, W. K. Gottschalk, S. S. Sundseth, T. A. Mansfield, R. K. Ramachandran, T. M. Willson, and S. A. Kliewer. 2001. Comprehensive messenger ribonucleic acid profiling reveals that peroxisome proliferator-activated receptor gamma activation has coordinate effects on gene expression in multiple insulin-sensitive tissues. *Endocrinology.* **142:** 1269–1277.

36. Elias, P. M., M. L. Williams, W. M. Holleran, Y. J. Jiang, and M. Schmuth. 2008. Pathogenesis of permeability barrier abnormalities in the ichthyoses: inherited disorders of lipid metabolism. *J. Lipid Res.* **49:** 697–714.

37. Demerjian, M., D. A. Crumrine, L. M. Milstone, M. L. Williams, and P. M. Elias. 2006. Barrier dysfunction and pathogenesis of neutral lipid storage disease with ichthyosis (Chanarin-Dorfman syndrome). *J. Invest. Dermatol.* **126:** 2032–2038.

38. Radner, F. P., I. E. Streith, G. Schoiswohl, M. Schweiger, M. Kumari, T. O. Eichmann, G. Rechberger, H. C. Koefeler, S. Eder, S. Schauer, et al. 2010. Growth retardation, impaired triacylglycerol catabolism, hepatic steatosis, and lethal skin barrier defect in mice lacking comparative gene identification-58 (CGI-58). *J. Biol. Chem.* **285:** 7300–7311.

39. Nimmo, H. G. 1979. Evidence for the existence of isoenzymes of glycerol phosphate acyltransferase. *Biochem. J.* **177:** 283–288.

40. Bates, E. J., and E. D. Saggerson. 1979. A study of the glycerol phosphate acyltransferase and dihydroxyacetone phosphate acyltransferase activities in rat liver mitochondrial and microsomal fractions. Relative distribution in parenchymal and non-parenchymal cells, effects of N-ethylmaleimide, palmitoyl-coenzyme A concentration, starvation, adrenalectomy and anti-insulin serum treatment. *Biochem. J.* **182:** 751–762.

41. Swanton, E. M., and E. D. Saggerson. 1997. Glycerolipid metabolizing enzymes in rat ventricle and in cardiac myocytes. *Biochim. Biophys. Acta.* **1346:** 93–102.

42. Lewin, T. M., H. de Jong, N. J. Schwerbrock, L. E. Hammond, S. M. Watkins, T. P. Combs, and R. A. Coleman. 2008. Mice deficient in mitochondrial glycerol-3-phosphate acyltransferase-1 have diminished myocardial triacylglycerol accumulation during lipogenic diet and altered phospholipid fatty acid composition. *Biochim. Biophys. Acta.* **1781:** 352–358.

43. Park, H., V. K. Kaushik, S. Constant, M. Prentki, E. Przybytkowski, N. B. Ruderman, and A. K. Saha. 2002. Coordinate regulation of malonyl-CoA decarboxylase, sn-glycerol-3-phosphate acyltransferase, and acetyl-CoA carboxylase by AMP-activated protein kinase in rat tissues in response to exercise. *J. Biol. Chem.* **277:** 32571–32577.

44. Stone, S. J., H. M. Myers, S. M. Watkins, B. E. Brown, K. R. Feingold, P. M. Elias, and R. V. Farese, Jr. 2004. Lipopenia and skin barrier abnormalities in DGAT2-deficient mice. *J. Biol. Chem.* **279:** 11767–11776.

45. Hammond, L. E., P. A. Gallagher, S. Wang, S. Hiller, K. D. Kluckman, E. L. Posey-Marcos, N. Maeda, and R. A. Coleman. 2002. Mitochondrial glycerol-3-phosphate acyltransferase-deficient mice have reduced weight and liver triacylglycerol content and altered glycerolipid fatty acid composition. *Mol. Cell. Biol.* **22:** 8204–8214.

46. Beigneux, A. P., L. Vergnes, X. Qiao, S. Quatela, R. Davis, S. M. Watkins, R. A. Coleman, R. L. Walzem, M. Philips, K. Reue, et al. 2006. Agpat6–a novel lipid biosynthetic gene required for triacylglycerol production in mammary epithelium. *J. Lipid Res.* **47:** 734–744.

47. Shan, D., J. L. Li, L. Wu, D. Li, J. Hurov, J. F. Tobin, R. E. Gimeno, and J. Cao. 2010. GPAT3 and GPAT4 are regulated by insulin-stimulated phosphorylation and play distinct roles in adipogenesis. *J. Lipid Res.* **51:** 1971–1981.

48. Lu, B., Y. J. Jiang, M. Q. Man, B. Brown, P. M. Elias, and K. R. Feingold. 2005. Expression and regulation of 1-acyl-sn-glycerol-3-phosphate acyltransferases in the epidermis. *J. Lipid Res.* **46:** 2448–2457.